Strain-free polished channel-cut crystal monochromators: a new approach and results

Elina Kasman*, Jonathan Montgomery, XianRong Huang, Jason Lerch, Lahsen Assoufid
Advanced Photon Source, Argonne National Laboratory, Lemont, IL USA

*ekasman@aps.anl.gov

ABSTRACT

The use of channel-cut crystal monochromators has been traditionally limited to applications that can tolerate the rough surface quality from wet etching without polishing. We have previously presented and discussed the motivation for producing channel cut crystals with strain-free polished surfaces [1]. Afterwards, we have undertaken an effort to design and implement an automated machine for polishing channel-cut crystals. The initial effort led to inefficient results. Since then, we conceptualized, designed, and implemented a new version of the channel-cut polishing machine, now called C-CHiRP (Channel-Cut High Resolution Polisher), also known as CCPM V2.0. The new machine design no longer utilizes Figure-8 motion that mimics manual polishing. Instead, the polishing is achieved by a combination of rotary and linear functions of two coordinated motion systems. Here we present the new design of C-CHiRP, its capabilities and features.
Multiple channel-cut crystals polished using the C-CHiRP have been deployed into several beamlines at the Advanced Photon Source (APS). We present the measurements of surface finish, flatness, as well as topography results obtained at 1-BM of APS, as compared with results typically achieved when polishing flat-surface monochromator crystals using conventional polishing processes.
Limitations of the current machine design, capabilities and considerations for strain-free polishing of highly complex crystals are also discussed, together with an outlook for future developments and improvements.

Keywords: Chemical-mechanical polishing, channel-cut crystal monochromator

1. INTRODUCTION

X-ray source properties continue to improve, bringing the expectations for optics to provide higher flux, lower scattering, and improved resolution. Historically, designers must choose between channel-cut monochromators, which offer the best mechanical stability but pollute the beam due to their rough, wavy surface, or separate monochromator crystals that can be produced with a highly polished diffracting surface, but require precision alignment. A new machine has been designed and built for automated polishing of channel-cut monochromators.

The C-CHiRP machine is fully functional, and five polished crystals have so far been successfully deployed into various beamlines of the APS. More machine design modifications are planned, and further polishing process development is needed to match channel cut crystal surface quality to that of flat polished double or single crystal monochromators. We discuss individual components of the machine, considerations for special features, and present surface finish and topography results from initial prototype runs. Software and automation setup and plans are briefly reviewed.

2. IMPLEMENTATION

2.1 Hardware

The major components of the C-CHiRP, shown on Figure 1 are: (1) rotary motor, (2) Z-stage, (3) linear stage for X-direction motion, (4) floating platform for loading with free weights resting on (5) linear bearings, (6) lifting fork, (7) interchangeable polishing tool, (8) drip tray, and (9) alignment stage for angular and Y-direction adjustment.

A Bison Gear™ AC rotary motor (1) with hardened steel worm-drive shaft and a forged bronze gear spins the polishing tool. This provides the necessary torque to sustain polishing friction for an extended time without overheating or stalling. A Vexta™ bi-slide linear stage driven by stepper motor (2) operated via VXM™ stepper motor controller serves as the Z-stage. An Aerotech ECO-165LM™ linear motor stage (3) ensures smooth polishing motion along the X-direction. The custom floating platform (4) rides on two vertical stainless shafts with linear bearings (5). This platform is lifted up and down using a custom lifting fork (5) attached to the Z-Axis (2). Disk-shaped polishing tools are made from aluminum or steel to match the geometry of each crystal. The polishing tool (7) is affixed to the swivel head, which in turn is connected to the motor shaft (1). A keyed shaft coupler ensures a rigid transfer of rotational speed regardless of the friction between the tool and crystal during polishing. In order to replace the polishing tool in-between steps, or for reconditioning, the platform is lifted out of the way using the Z-stage fork. A drip tray (8) contains the sludge slurry and drains the waste into a collection bucket (not shown). Another important component is the alignment stage (9), which allows for both a theta alignment and fine adjustment of position in the Y-direction. This fine adjustment is necessary to ensure that the bottom of the crystal channel moves parallel to the edge of the polishing tool, and as close to full depth as possible. The goal is to achieve an exclusion area no wider than a millimeter, maximizing the clear aperture of the polished surfaces. The channel-cut crystal rests on its outer side wall, surrounded by outriggers chosen to match the crystal's channel wall thickness. These pieces are mounted with a thermoplastic adhesive to a ceramic block which is then securely clamped into the tray. Additional supporting blocks are necessary for channel-cut crystals with bottom mounting flanges.

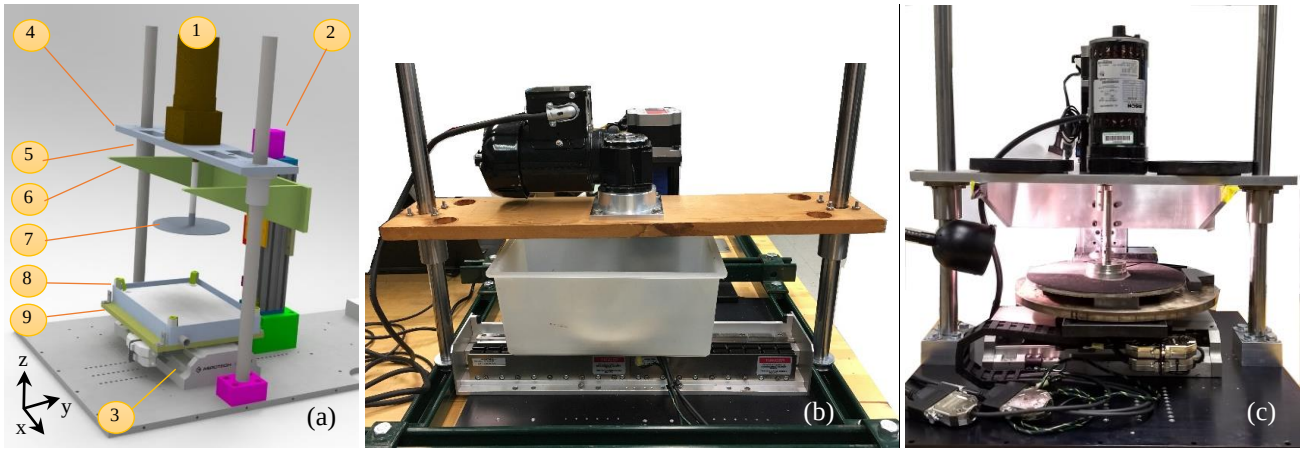

Figure 1. (a) Machine model, (b) photo of early prototype, and (c) final commissioned C-CHiRP machine during initial trial runs, before the installation of alignment stages. Major components are: 1) rotary motor with gearhead (straight motor shown in model and photo of C-CHiRP, right angle motor shown in photo of prototype); 2) Z-stage; 3) linear stage for X-direction motion; 4) floating platform, 5) vertical rods with linear bearings for floating the platform, 6) lifting fork, 7) interchangeable polishing tool, 8) drip tray, 9) alignment stage for angular and Y-direction adjustment.

2.2 Software

The Z-stage motor is controlled via a one axis programmable stepper motor controller, capable of continuous and jog motions at set step size. USB to RS232 serial communication port allows for future controls integration. The Rotary motor is operated via an on/off switch on the motor power cord, to be replaced by a remotely controllable relay. Linear motion of the horizontal linear stage is driven by the Aerotech Soloist™ module controlled by Ensemble software®. All three of these systems will combine into a monolithic control system using the Ensemble software backbone.

2.3 Tooling and fixtures

During the planarization lapping and polishing steps, we affix various polishing pads to the bottom of the disc-shaped tool. The crystal channel geometry varies: crystals come in different depth and width of the channel. The disc tool itself also has numerous properties that are dependent on the channel geometry. These parameters are the disc thickness, disk radius, material, and penetration depth. 'Free' weights can be added on top of the floating platform, provide the

controlled down-force required for efficient polishing process. This force is translated to the polishing tool via the motor shaft and swivel head mounted to the center of the polishing tool, creating an uneven pressure distribution and a tendency to deform the tool. Outrigger crystals are used to support the tool away from the active surface, providing a more uniform pressure distribution. However, because the polishing tool is ultimately a thin solid disc, it will have a tendency to deform due to the elasticity of the tool material. Our goal is to minimize this deformation by designing the polishing tool with optimal rigidity, maximizing polished crystal flatness. We approach the tool design iteratively. First, we assume thickness, radius, material and penetration depth parameters based on the geometry of the channel-cut crystal. Then, we calculate the maximum deformation at infinite time of polishing. Because the crystal surface directly mirrors the shape of the polishing tool, this calculation gives us the worst-case scenario for potential crystal flatness due to uneven polishing with a deformed tool. Experimentation has shown that there is little concern that this deformation will at any time cause the top of the disc tool to bind the disc on the top surface of the crystal channel.

Roark's Formulas for Stress and Strain[2] are used to model the circular plate uniformly loaded in the center. Tool bending labels and definitions to calculate the asymptotic tool deformation at infinite polishing time and worst-case scenario crystal slope are shown below in Figure 2. The following assumptions must be met in order to use the equations described below: the plate is flat, of uniform thickness, and of homogeneous isotropic material; the thickness is not more than one-quarter of the smallest transverse dimension; all forces (loads and reactions) are normal to the plane of the plate; the plate is nowhere stressed beyond its elastic limit.

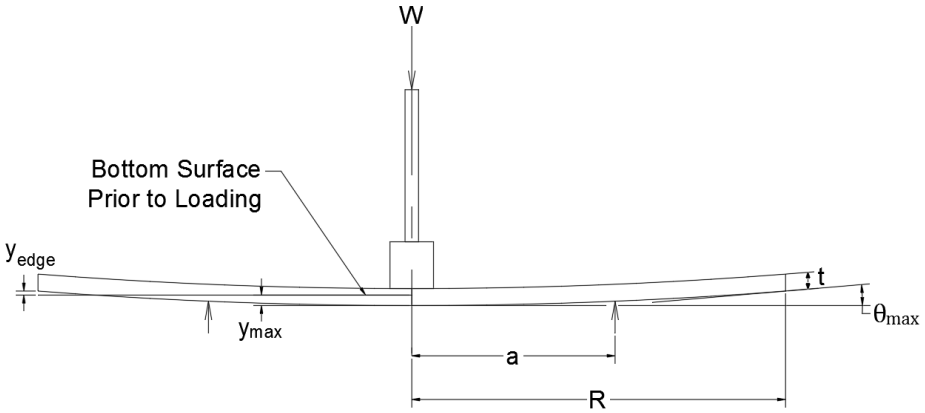

Figure 2. Tool bending labels and definitions to calculate asymptotic tool deformation and worst-case scenario crystal slope.

The maximum center deflection y_{max}, and maximum edge slope θ_{max} can be found by solving equations 1and 2:

$$y_{max} = \frac{-Wa^2(3+\nu)}{16\pi D(1+\nu)} \qquad (1)$$

$$\theta_{max} = \frac{Wa}{4\pi D(1+\nu)} \qquad (2)$$

In Equation 1 and 2, ν represents Poisson's ratio (a material property), and D is a relationship described below in equation 3 known as the flexural rigidity:

$$D = \frac{Et^3}{12(1-\nu^2)} \qquad (3)$$

In equation 3, E represents the Young's modulus (elastic modulus) for the material. Also, in equation 1 the maximum center deflection occurs along the center axis, while in equation 2 the maximum slope occurs at distance a from the center axis.

Although we mathematically model the disc edges as being simply supported, the physical reality is that the edge of the disc extends beyond the support. Two considerations need to be resolved for this scenario. First, the bending moment

created by a portion of the disc cantilevering beyond the support point. The resulting bending moment from the cantilever is negligible given the small force from the weight of the cantilevered disc relative to the force pressing down on the center of the disc. The second consideration is the maximum vertical deflection of the disc edge. Equation 4 is used to determine the maximum vertical deflection of the outside disc edge:

$$y_{edge} = (R - a)\tan(\theta_{max}) \qquad (4)$$

We calculate maximum vertical deflection for both aluminum and 304 stainless steel tools (304 SST), the two materials most commonly available for rapid manufacturing, using fixed dimensions of our swivel head as tool support chuck. These values are presented in Table 1. As expected, to minimize tool deflection, the most rigid material is the best choice for the polishing disk tool. We design the polishing tool to maximum thickness that comfortably fits inside the crystal channel width. Tool thickness must also accommodate for the thickness of the polishing and cushioning pads mounted on the bottom and top surfaces of the tool.

Table 1. Example of calculated asymptotic polishing tool deflection. These values are used to select most suitable polishing tool material and decide if adjustment of tool geometry is necessary.

Crystal Channel *[mm]*		Polishing tool geometry				y_{edge} *[μm]*	
Depth	*Width*	*a [mm]*	*R [mm]*	*t [mm]*	*W [lbf]*	Aluminum	304 SST
76	8	105	28	4	60	83	32
76	8	105	28	4	40	56	21
8	4	34	26	2	20	21	8
12	20	50	12	8	40	1.5	0.56

Outriggers are selected to be of the same height as the crystal surface being polished. The collective top surface of all the outriggers combined creates the plane upon which the polishing tool rides, defining the resulting flatness of the polished crystal diffractive surface. By adjusting the relative height of outriggers positioned around the inner surface of channel-cut crystal, the parallelism and wedge of diffracting surfaces can be slightly corrected. The polishing tool has a swivel joint connection for angular correction adjustments, allowing it to fully mate with the collective top surface of the outriggers and the slotted crystal combined.

3. RESULTS AND DISCUSSION

The polished crystal surfaces are evaluated by measuring roughness and flatness. Both quaities have a direct effect on beam scattering, especially at low incidence angles, as well as, affecting the preservation of coherence in more sensitive applications. Beam distortions could result from the subsurface damage remaining after machining steps, and crystal strain remaining after various lapping and polishing steps. White beam topography and contrast feature studies are used as a visual qualifier. As the incoming bulk crystal quality is known to be “perfect” without dislocations, slips, voids, or other crystalline defects, any contrast or features in topography images indicate subsurface damage or strain resulting from machining or lapping steps that were not removed in the polishing step. Normally, in a well-balanced and properly designed finishing process, each subsequent fabrication step will completely remove any damage remaining from the preceding machining or abrasive step. Subsequent abrasive processing step introduces its own subsurface damage and strain, which, under normal circumstances, should be significantly lower than the previously present damage. If the polishing step is not well balanced, additional scratches or defects might be introduced. These will show up on either roughness or topography images, indicating that further process development and adjustment is necessary.

The surface roughness achieved using the C-CHiRP machine was compared with typical results after similar process using conventional plano polishing tools. For the C-CHiRP results, the equivalent measurements were taken from crystal outriggers, due to the physical inaccessibility of the internal diffracting surfaces. Directional surface features, aligned with the rotation of the tool, are clearly visible in Figure 3 (a), the C-CHiRP result. This means mechanical and chemical components of the CMP step were not well balanced. To correct this issue we need to look at the kinematics of rotation vs. linear motion, and dwell times, as well as concentration of polishing slurry. We could also consider adding an intermediate pre-polishing step using finer abrasive slurry to minimize surface and subsurface damage after the planarization lapping abrasive step, potentially shortening the overall CMP time and thus reducing the effect of the chemo-mechanical imbalance.

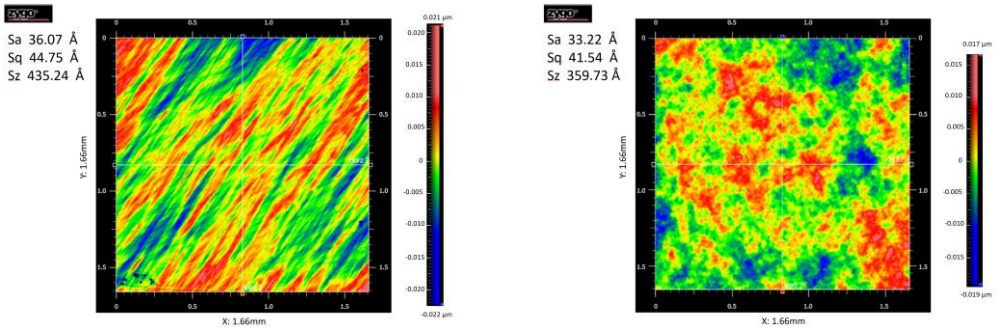

(a) (b)

Figure 3. Roughness of polished crystal surfaces. (a) Result after polishing using C-CHiRP machine as compared with (b) surface roughness after conventional flat crystal polishing. While average and RMS roughness numbers, Sa and Sq, are comparable, the C-CHiRP polished surface clearly shows directional surface features aligned with rotation of the tool.

The orientation of the evaluated polished Si crystal surfaces are (111). Synchrotron white-beam topography of these surfaces was carried out at the APS bending-magnet beamline 1-BM in the reflection geometry with the incidence angle being around 5 degrees. The Bragg reflection of the selected Laue spot is -13-1 with diffraction X-ray wavelength being around 0.57 angstroms (E = 21.7 keV). Contrast features captured in topography images in Figure 4 correspond to subsurface damage remaining after the polishing process. Both polished channel cut crystals performed sufficiently well when deployed at their respective beamlines. More work is needed to improve the polishing process in order to achieve truly subsurface damage-free and strain-free crystal surfaces.

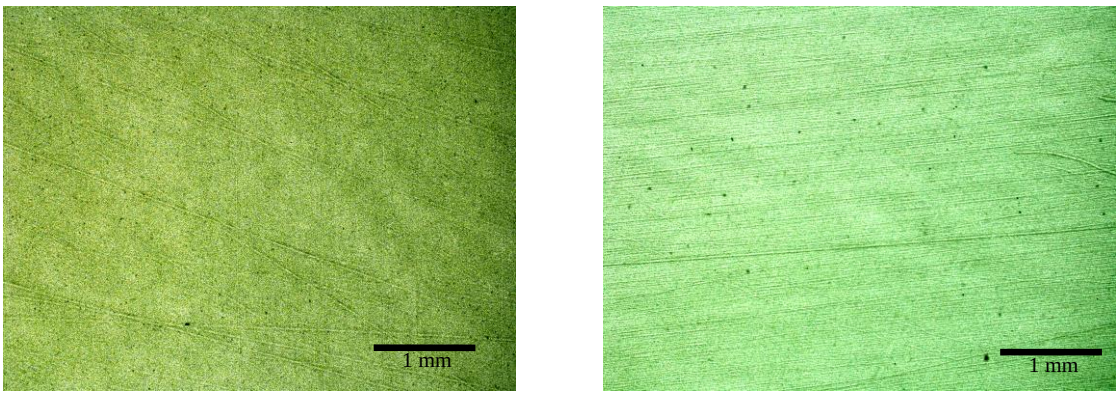

(a) (b)

Figure 4. White beam topography carried out at 1-BM beamline of APS shows some contrast corresponding with polishing. Despite the slight defects, both crystals (a) and (b) performed well at 14-ID-D and 27-ID beamlines, respectively.

Parallelism of inner surfaces becomes increasingly important for multi-bounce applications. One such example is a long and deep crystal, where a manual polishing attempt has been previously unsuccessful. Measurements of inner surfaces of the deep slotted crystal are shown in Figure 5. There is an obvious (c) wedge between the Left and Right side of the inner slotted crystal walls, as well as, a (c) concave shape to both surfaces, remaining after previous manual polishing attempts. The wedge can be corrected by selecting the outriggers placed opposite the bottom of the channel to be slightly taller than the side wall thickness, swiveling the polishing tool downward so that it takes material off more aggressively towards the bottom of the channel.

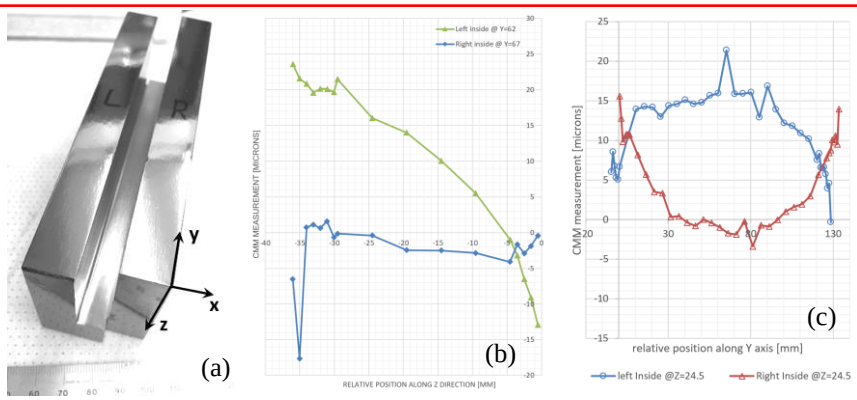

Figure 5. Parallelism and flatness of inner channel surfaces of deep long slotted crystal. Measurements were taken on Brown & Sharpe CMM with a ruby tip. Sharp surface measurement transitions (c) demonstrate scratches. This contact measurement method may not be suitable for final polished crystals due to risk of scratches.

4. FUTURE WORK

The instrument has been shown to be functional and productive, however full integration of all motion components under a monolithic controls system is required. Development of a polishing process that will produce fully strain-free and scratch-free surface of inner channel walls by exploring a matrix of polishing consumables, choice of abrasives and duration of each polishing step is the subject of an ongoing study. Modeling the material removal rate for each crystal surface point based on effective abrasive concentration and tool speed will be helpful to develop the most efficient linear/rotational motion algorithm to optimize flatness and parallelism of the diffracting surfaces.

Proper slurry delivery to each surface point to reduce or eliminate slurry starvation at the center of the polishing tool is important to extend uninterrupted polishing time between pad surface cleanings and pad reconditioning. By improving slurry delivery, overall efficiency of the polishing steps will be higher, and also lead to a reduction in human involvement and handling.
We intend to explore methods for non-contact measurements of inner channel walls which will serve as direct feedback for iterative surface improvements.

ACKNOWLEDGEMENTS

EK would like to thank S. Bean of APS engineering group for mechanical design work on the alignment stage. EK and XH are grateful to A. T. Macrander at beamline 1-BM of APS for great help in the white-beam topography work. This work was supported by the US Department of Energy, Office of Science, Office of Basic Energy Sciences, under contract No. DE-AC-02-06CH11357.

REFERENCES

[1] E. Kasman, et. al. “The best of both worlds: automated CMP polishing of channel-cut monochromators”, Proc. SPIE 9590, Advances in Laboratory-based X-Ray Sources, Optics, and Applications IV, 95900D (September 3, 2015); doi:10.1117/12.2196034.
[2] Young, Warren C., and Raymond J. Roark. "Chapter 11: Flat Plates." Roark's Formulas for Stress and Strain. 7th ed. New York: McGraw-Hill, 2002. 429+. Print page 491.